

SEBS/PPy.DBSA Blends: Preparation and Evaluation of Electromechanical and Dynamic Mechanical Properties

D. Muller,¹ M. Garcia,¹ G. V. Salmoria,¹ A. T. N. Pires,² R. Paniago,³ G. M. O. Barra¹

¹Mechanical Engineering Department, LABMAT, Florianópolis, Santa Catarina, Brazil

²Chemistry Department, POLIMAT Federal University of Santa Catarina, Campus Universitário 88040-900 Florianópolis, Santa Catarina, Brazil

³Physics Department, Federal University of Minas Gerais, Belo Horizonte, Minas Gerais, Brazil

Received 24 February 2010; accepted 4 August 2010

DOI 10.1002/app.33141

Published online 13 October 2010 in Wiley Online Library (wileyonlinelibrary.com).

ABSTRACT: In this study, the electromechanical and dynamic mechanical properties of electrically conducting polymer blends were investigated. The blends were comprised poly(styrene-*b*-butylene-*ran*-ethylene-*b*-styrene) (SEBS) containing polypyrrole doped with dodecylbenzenesulfonic acid (PPy.DBSA). The two types of PPy.DBSA (with and without an excess of DBSA) were blended with SEBS through the solution casting method at room temperature. The dynamic mechanical characterization of the SEBS/PPy.DBSA blends demonstrated that the use of PPy.DBSA with and without free DBSA molecules results in different

degrees of interaction with the two phases of the SEBS copolymer matrix. The changes in the electrical conductivity of the blends during repeated pressure loading/unloading were investigated. The conducting SEBS/PPy.DBSA polymer blends exhibited an increase in the electrical conductivity on pressure loading and underwent a corresponding decrease on unloading. © 2010 Wiley Periodicals, Inc. *J Appl Polym Sci* 120: 351–359, 2011

Key words: polypyrrole; electromechanical properties; thermoplastic elastomer

INTRODUCTION

Blends of intrinsically conducting polymers (ICP) and insulating polymers constitute a class of conducting materials which can present attractive mechanical properties and electrical conductivity with excellent processability. New technological applications are being found for these materials, such as electromagnetic shielding,¹ optoelectronic displays,² chemical sensors,³ biosensors,⁴ and electromechanical sensors.^{5–8}

Considerable efforts have been made to develop electromechanical sensors with fast and linear response, reliability, high reproducibility, and low cost. Blends with rubber as the matrix and ICP as the disperse phase are very attractive systems for use in electromechanical sensors, due to the mixture of these components offering flexibility, stress/strain recovery characteristics, and controlled levels of electrical conductivity. The mechanical sensitivity of conducting polymer blends is dependent on the test conditions, such as temperature and the compressive

or tensile forces applied. Under compressive force, the electrical conductivity rises due to an increase in the contact of the conducting filler, i.e., the arrangement of ICP particles, and a conducting pathway is formed. When the compressive force is released, the conducting pathway is discontinued, reducing the electrical conductivity to a value corresponding to that without compression force.^{9,10} Alternatively, there are other systems, such as carbon black (CB) composites, in which the electrical conductivity decreases when compressive forces are applied.^{10,11} This behavior has been attributed to the destruction of the conducting CB network. Some unsaturated rubbers, such as poly(*cis*-1,4-isoprene) (PIP),⁷ polyurethane (PU),⁸ natural rubber (NR),¹² nitrile rubber (NBR),^{13,14} silicone rubber,^{15,16} and thermoplastic rubbers,^{17–20} have been used as matrices to obtain conducting elastomeric blends.

Polypyrrole (PPy) has been used extensively as a conducting filler in polymer blends due to its good environmental, thermal stability, and electrical properties. However, PPy is usually immiscible when blended with rubbers, and gross phase separation processes may restrict the formulation of compatible materials. The compatibility of conducting polymer blends was enhanced through inserting counter ions, such as dodecylbenzenesulfonic acid (DBSA), into the PPy chains, making it possible to form blends compatible with an insulating polymer. Blends of polypyrrole doped with dodecylbenzenesulfonic

Correspondence to: G. M. O. Barra (guiga@emc.ufsc.br).

Contract grant sponsors: Brazilian government agencies Conselho Nacional de Desenvolvimento Científico e Tecnológico (CNPq), Coordenação de Aperfeiçoamento de Pessoal de Nível Superior (CAPES).

acid (PPy.DBSA) and rubbers prepared through the solution casting method have been reported to be quite efficient when both polymers are soluble in a common solvent.²¹ The conductivity of solution-cast blends is dependent on the ability of the PPy to finely disperse in the solvent and its compatibility with the rubber solution.

The focus of this study was to evaluate the effect of the PPy.DBSA characteristics, such as doping degree and DBSA concentration, on the morphology, electrical conductivity, and dynamic mechanical and electromechanical properties of conducting blends. To this end, PPy.DBSA samples with and without an excess of DBSA were mixed separately with poly(styrene-*b*-butylene-*ran*-ethylene-*b*-styrene) (SEBS) through the solution casting process.

EXPERIMENTAL

Materials

Pyrrole (analytical grade, Merck) was distilled twice under vacuum and stored in a refrigerator. Ammonium persulfate (APS) (analytical grade, Merck), and DBSA (technical grade, Pro-Química do Brazil) were used without purification. The polymer used in this study was a block copolymer with styrene hard segments and ethylene-butadiene rubbery segments. The copolymer poly(styrene-*b*-butylene-*ran*-ethylene-*b*-styrene) (SEBS), commercially designated Kraton G1652, was kindly supplied by Shell Química (Brazil). The number average molecular weight of Kraton G 1652 is 54,000 g mol⁻¹ (according to the supplier), with a polystyrene block content of 30 wt %.

Synthesis of PPy.DBSA

The polymerization of pyrrole was performed as described by Lee et al.²² First, 0.15 mol of DBSA were dispersed in 500 mL of distilled water under stirring and 0.3 mol of pyrrole was added. The mixture was then stirred for 20 min, at 5°C, following which 0.06 mol of ammonium persulfate (APS) dissolved in 100 mL water was slowly added, and the reaction mixture was stirred for 24 h. The reaction mixture was precipitated in acetone, and the precipitate was filtered, washed with acetone and dried in an oven at room temperature, and a black powder was formed with 30% yield. The PPy.DBSA samples washed with acetone were denoted as PPy.DBSA-W1. To remove the excess DBSA, PPy.DBSA-W1 samples were stirred in distilled water for 24 h, filtered, washed with distilled water, and dried. These samples were denoted as PPy.DBSA-W2. The doping degrees of PPy.DBSA-W1 and PPy.DBSA-W2 were determined through X-ray photoelectron spectroscopy (XPS).

Preparation of blends

Toluene solutions of PPy.DBSA-W1 or PPy.DBSA-W2 at 2% w/v and SEBS at 10% w/v were mixed in different compositions and stirred for 3 h. The solutions were cast on glass plates to evaporate the solvent at room temperature, obtaining films with thicknesses of 300–350 μm.

Characterization

The XPS measurements of the polymer samples were obtained using a VG ESCALAB 220i - XL spectrometer with an Al K-α X-ray source (1486.6 eV) operating at 150 W. The electron analyzer equipped with 5 channel trons was operated at fixed pass energy of 50 eV for the survey spectra and 20 eV for the N-1s and C-1s spectra. To compensate for surface charging effects, all binding energies (BEs) were referenced to the C-1s neutral carbon peak at 284.6 eV. The area ratio corrected by the sensitivity factor was used for quantitative analysis of the XPS data.

Perkin-Elmer UV-Vis (Lambda 16) spectrometer was used to obtain the spectral features of the PPy.DBSA samples. The surfaces of the thin films were studied by optical microscopy, on an Olympus BX50 optical microscope at 200 × magnification.

The dynamic mechanical properties of the blends and SEBS were studied using a dynamic mechanical analyzer (DMA-983 interfaced to a TA 2000). The DMA measurements were carried out in a nitrogen gas environment, at a heating rate of 5°C min⁻¹ and at 1, 10, 30, and 50 Hz with a single cantilever.

The electrical conductivity values of the blends and undiluted components were determined using the two-probe standard method with a Keithley, Model 6220, current source to apply the current and a Keithley, Model 6517, electrometer to measure the potential difference. The conductivity was calculated through eq. (1), where d is the electrode diameter (cm), w is the specimen thickness (cm), and I and V are the applied current and voltage measurement, respectively.

$$\sigma = \frac{4wI}{\pi Vd^2} \quad (1)$$

Measurements of the electrical conductivity of the blends on pressure loading/unloading were performed using the system schematized in Figure 1. Small strips of conducting blends with a diameter of 24.5 mm and 100–300 μm thickness were placed between two metallic electrodes which were confined to a special poly(tetrafluoroethylene) cylinder. The electrodes were connected to a Keithley, Model 6220, current source to apply the current (1 nA to 0.1 mA), and a Keithley, Model 6517, electrometer to

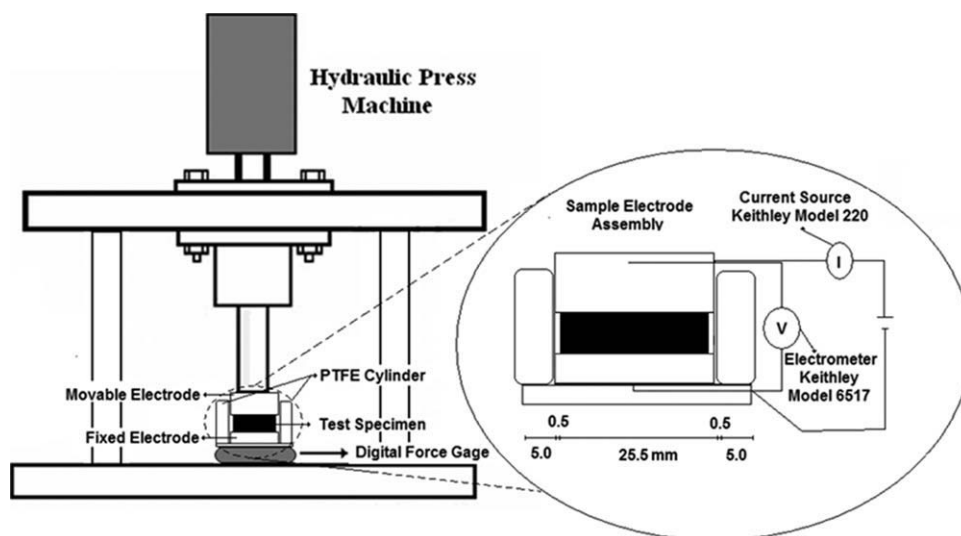


Figure 1 Experimental device for the electrical mechanical measurements.

measure the potential difference. A digital force gauge (MK Instruments) connected to a microprocessor was used to measure the compression force. A continuous conductivity response curve with the application and removal of a mechanical load was plotted. All specimens were electrically isolated from the mechanical testing fixtures and loaded at 10 MPa for 90 s. The pressure was removed and the unloaded state was also maintained for 90 s. Sequences of 10 cycles were performed on each sample.

RESULTS AND DISCUSSION

The structure of the PPy highly doped with DBSA schematized in Figure 2 contains 0.33 positive charges per monomer unit.²³ The doping degree of the PPy.DBSA used in this study was determined from XPS analysis by calculating the amount of different neutral and positive nitrogen species of the PPy chain from the properly curve-fitted N-1s core-level spectrum. The PPy.DBSA-W1 samples, as shown in Figure 3(a), exhibit four peaks related to the nitrogen atom. The peak with BEs at 399.5 eV is related to amine groups.²³ The peak at 398.2 eV is related to imine group in the macromolecule chain, probably formed due to the overoxidation process during the polymerization reaction, as described in the literature.²⁴ The two peaks with BEs at 400.8 and 402.3 are attributed to the positively charged nitrogen, according to reports in the literature.^{23,24} The proportion of charged nitrogen (N^+) was around 0.36, which corresponds to the doping degree. PPy.DBSA-W1 recovered from the acetone medium was washed with water to verify the effect of the purification process on the doping level and electrical conductivity value, obtaining a sample denoted

as PPy.DBSA-W2. From the analysis of the N-1s peak, in Figure 3(b), the proportion of charged nitrogen in the PPy.DBSA-W2 sample was around 0.33.

Table I summarizes the surface elemental analysis of the PPy.DBSA-W1 and PPy.DBSA-W2 samples, where the doping degree and conductivity values of the PPy.DBSA samples do not present a significant decrease after washing with water. However, the solubility of PPy.DBSA-W2 in organic solvents, such as toluene, chloroform, and *m*-cresol, was lower than that of PPy.DBSA-W1.

The amount of DBSA present as the molecular species can be calculated from the difference between the S/N molar ratio and the proportion of positively charged nitrogen ($S/N - N^+$). In general, PPy highly doped with DBSA contains theoretical S/N and C/N ratios of around 0.33 and 10.0, respectively. The ratios of S/N and C/N for PPy.DBSA-W1 are higher than the theoretical values, indicating that a considerable amount of molecular DBSA is present in the sample. The difference between the value for the S/N molar ratio (0.63) and the positively charged nitrogen (0.36) corresponds to an excess of DBSA in the range of 0.27 mmol. On the other hand, PPy.DBSA-W2 has molar ratios very close to the theoretical values, indicating that all the DBSA is bound to the carbon site of the quinoid rings, forming π electron radicals on the PPy macromolecules.

The UV-Vis spectra of the PPy.DBSA samples presented absorption bands at 345 nm and 475 nm, corresponding to the energy to π - π^* transition of the π electrons of the neutral pyrrole trimer, and the oxidized form.

Figure 4(a) shows the variation in the storage modulus (E') as a function of temperature, for undiluted SEBS and SEBS/PPy.DBSA blends. A sudden fall in the storage modulus is observed for undiluted

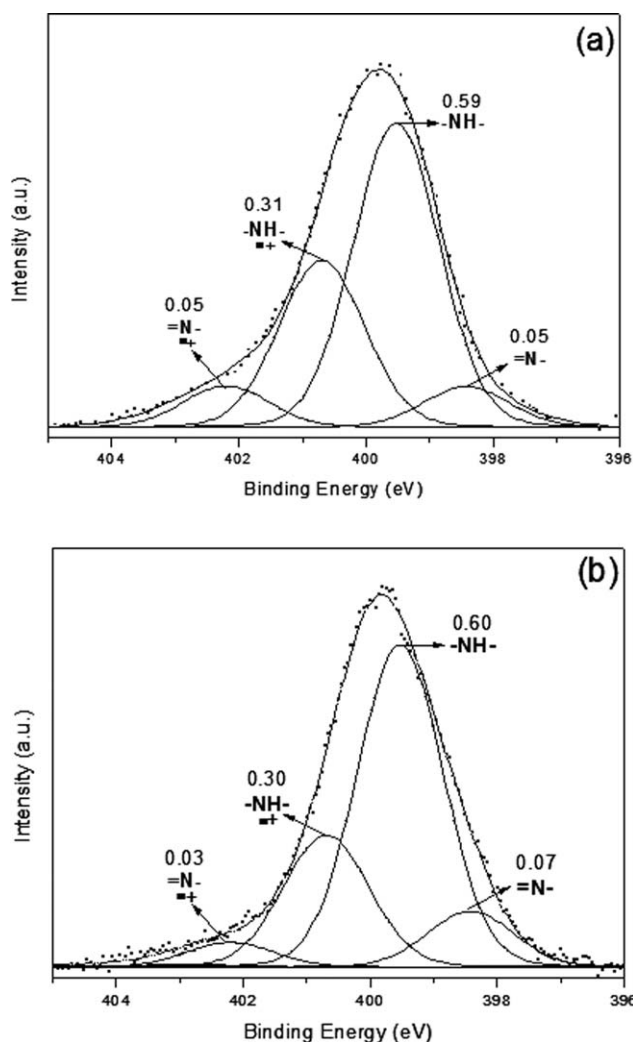


Figure 2 Chemical structure of polypyrrole doped with dodecylbenzenesulfonic acid (PPy.DBSA).

SEBS at -36°C , which corresponds to the glass-rubber transition of the ethylene-ran-butylene segments of the SEBS triblock copolymer. As expected, the storage modulus values for the blends are higher than those for the undiluted SEBS over the whole temperature range evaluated. Below the glass-rubber transition temperature of the rubber segments, a slight increase in the modulus was observed for the blends when compared with the undiluted SEBS. However, the blends exhibit a marked increase in

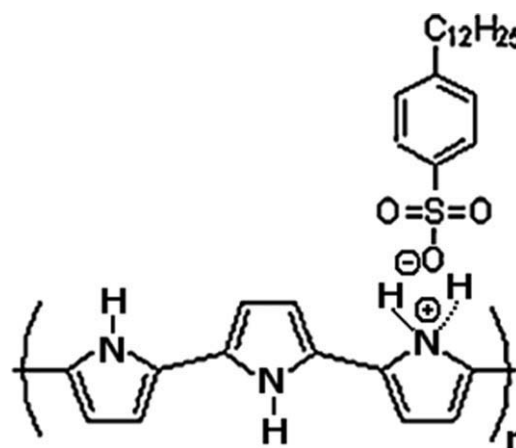


Figure 3 Nitrogen 1s (N-1s) XPS core-level spectrum of (a) PPy.DBSA-W1 and (b) PPy.DBSA-W2 samples.

the storage modulus in the rubbery region (up to -36°C), compared with the glass region. This behavior is similar to those found when CB^{11,25} is used as the conducting filler in composite systems. The rigidity of the blend increases due to the presence of conducting agglomerates, which restricts the mobility of the matrix polymer chains. It was noted, that the storage modulus values for the SEBS/PPy.DBSA blends were affected by the PPy/DBSA ratio of the PPy.DBSA-W1 and PPy.DBSA-W2 composition, as can be seen in Figure 4(a).

Figure 4(b) shows the loss tangent ($\tan \delta_{\max}$) of the blends and undiluted SEBS as a function of temperature. The two glass transition temperatures at -36°C and 96°C , corresponding to the ethylene-ran-butylene and styrene segments, respectively, are not affected by the presence of PPy.DBSA-W1 or PPy.DBSA-W2. The peak intensity, corresponding to the glass transition temperature of ethylene-ran-butylene and styrene blocks, reduces on increasing the amount of conducting polymer, but due to the presence of a DBSA excess in the PPy.DBSA-W1, acting as the plasticizing agent, the variation in the $\tan \delta_{\max}$ value is lower for SEBS/PPy.DBSA-W1 than for SEBS/PPy.DBSA-W2 blends. These changes in the magnitude of the loss tangent are related to the incorporation of PPy.DBSA, which reduces the flexibility of the EB and styrene blocks.

TABLE I
Electrical Conductivity, Doping Degree and Area Ratio (atom %) of Elemental Composition of PPy.DBSA-W1 and PPy.DBSA-W2 Samples Obtained from the Wide XPS Scans

Samples	Doping degree (%)	Electrical conductivity (S cm^{-1})	Area ratio (atom %)				Molar ratio		
			C	N	S	O	C/N	S/N	S/N - N ⁺
PPy.DBSA-W1	36	0.34	71.8	5.2	3.3	19.7	13.8	0.63	0.27
PPy.DBSA-W2	33	0.46	71.3	6.8	2.3	19.6	10.5	0.34	0.01

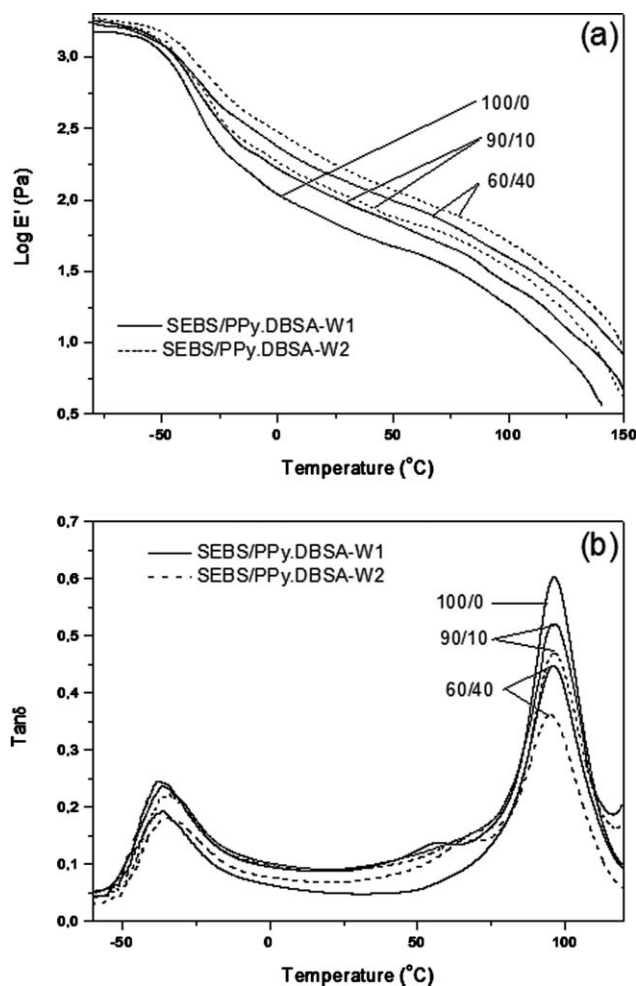


Figure 4 Dependence of (a) bending modulus and (b) $\tan \delta$ on temperature for undiluted SEBS and its blends with 10 and 40 wt % of PPy.DBSA-W1 or W2.

According to Leyva et al., the heterogeneous distribution of the conducting polymer in one preferential phase of a triblock copolymer can be estimated using the normalized curve of $\tan \delta / \tan \delta_{\max}$ versus T/T_{\max} . The $\tan \delta$ represents the loss tangent values at any temperature T and the $\tan \delta_{\max}$ represents the loss tangent value at the corresponding T_{\max} temperature.^{25,26} The extent of broadening of the normalized plots in the relaxation process of a specific phase can be correlated to the presence of the conducting additive inside this phase.²⁷

Figures 5 and 6 show the normalized curves for SEBS/PPy.DBSA-W1 and SEBS/PPy.DBSA-W2, respectively, at frequencies of 1 and 50 Hz. For SEBS/PPy.DBSA-W1, there is broadening of the normalized curves for the PEB and PS phase transitions with increasing conducting filler, indicating that the PPy.DBSA is distributed in both phases. The PEB phase relaxation curves are coincident for all blend compositions in the SEBS/PPy.DBSA-W2 blends, with no difference in the broadening. On the other

hand, the width of these curves for the PS phase enhanced with increasing conducting polymer concentration, suggesting that PPy.DBSA-W2 is preferentially distributed in the PS phase. These results indicate that DBSA acts as a compatibilizing agent, promoting a better compatibility with the PS and PEB phases in the SEBS matrix.

The activation energy (E_a) values related to the relaxation processes for each blend composition were determined from the temperature corresponding to the $\tan \delta_{\max}$ taken at different measurement frequencies, using the Arrhenius equation [eq. (2)]. These values are related to the interaction between the conducting filler and the phases of the copolymer matrix.²⁷

$$f = f_0 e^{-E_a/RT} \quad (2)$$

where f is the frequency used in the experiment and T is the corresponding temperature at the damping peak maximum, that is, the glass transition temperature T_g .

The activation energy values, calculated through the plot of $\log f$ versus $\log 1/T$ for the relaxation of PEB and PS (Table II), are consistent with the discussion on the normalized curves, where only the PEB phase in the SEBS/PPy.DBSA-W2 blends has the same E_a values. These results are similar to those obtained for SBS/PAni.DBSA and SBS/EB (emeraldine base) blends.²⁵

The dependence of the electrical conductivity on the blend composition is shown in Figure 7 for SEBS/PPy.DBSA-W1 and SEBS/PPy.DBSA-W2. As expected, the electrical conductivity values increase with increasing amount of PPy.DBSA in the insulation SEBS matrix. For 20 and 40 wt % of PPy.DBSA-W1, the electrical conductivity values were 1.1×10^{-5} and 3.1×10^{-4} S cm⁻¹, respectively, which are 10⁶- and 10⁷-fold higher than the values for the undiluted SEBS. Furthermore, SEBS/PPy.DBSA-W2 blends displayed lower electrical conductivity values than SEBS/PPy.DBSA-W1 in all blend compositions studied.

The data presented in Figure 7 can be fitted to the scaling law of percolation theory²¹ K. Levon, as described in eq. (3)

$$\sigma_f = c(f - f_p)^t \quad (3)$$

where c is a constant, t a critical exponent, σ_f the conductivity, f the fraction of the conductive medium and f_p the fraction at the percolation threshold expressed as a weight fraction.

The values for the critical exponent and percolation threshold were 2.6 and 3 wt % for SEBS/PPy.DBSA-W1, and 4.1 and 10 wt % for SEBS/PPy.DBSA-W2, respectively. The values for the

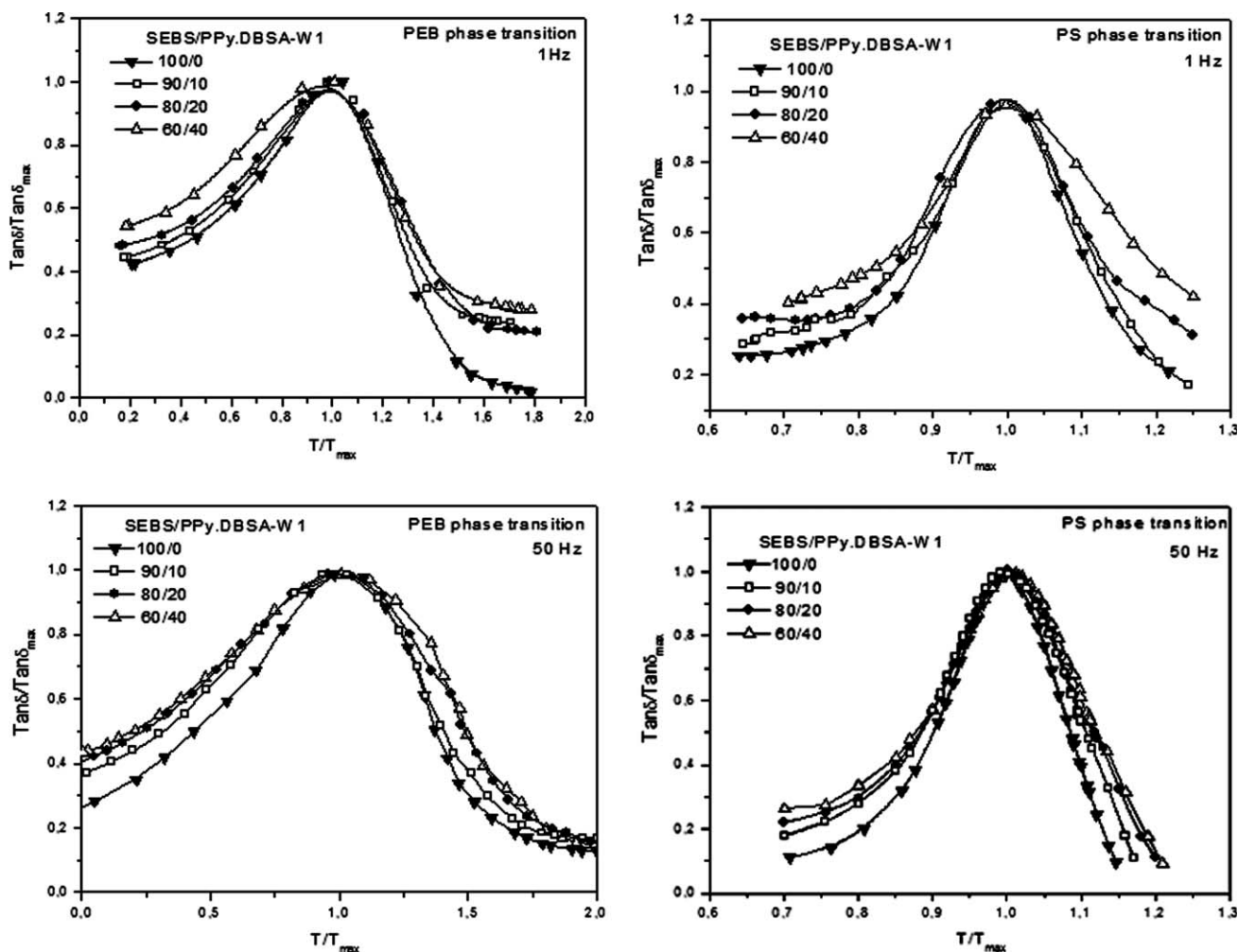


Figure 5 Normalized curves of $\tan \delta / \tan \delta_{\max}$ versus T/T_{\max} at 1 and 50 Hz for PEB and PS phase relaxations in undiluted SEBS and in SEBS/PPy.DBSA-W1.

critical exponent were in the range of 2-4, which can be explained by multiple percolation in the conducting polymer blends, as proposed by Levon and Margolina.²⁸ The lower f_p value for SEBS/PPy.DBSA-W1 reflects a lower compatibility of the components in this blend, since the presence of DBSA in excess increases the electrical conductivity of the blend. These results are consistent with those obtained in the morphological and dynamic mechanical analysis.

The microstructure of the SEBS/PPy.DBSA blends revealed typical phase separation morphology with the presence of PPy.DBSA agglomerates (the dark regions seen in the optical micrograph of the insert in Fig. 7). SEBS/PPy.DBSA-W1 blends [Figs. 7(A,C)] presented disperse agglomerates composed of conducting pathways, with the disperse phase better interconnected compared to the SEBS/PPy.DBSA-W2 blends [Figs. 7(B,D)]. The microstructure of the SEBS/PPy.DBSA-W1 blends indicates that the DBSA excess was able to improve the distribution of the conducting polymer agglomerates in the SEBS ma-

trix, and consequently improve the electrical conductivity values.

The relative conductivity ($\Delta\sigma$) was calculated according eq. 4, where σ_s is the electrical conductivity under compressive stress and σ_0 is the electrical conductivity for the original shape. The ratio between the relative conductivity and the compressive stress variation is defined as the compression sensitivity.¹⁹

$$\Delta\sigma = \frac{(\sigma_s - \sigma_0)}{\sigma_0} \quad (4)$$

The SEBS/PPy.DBSA-W1 blends showed a change in the relative conductivity values as a function of compressive stress, as can be seen in Figure 8. For a filler content below 20 wt %, there is no significant increase in the relative conductivity during the electromechanical assay. Under these conditions, deformation of the blend specimen at constant temperature due to applied compressive stress can decrease slightly the PPy.DBSA agglomerate distances, and

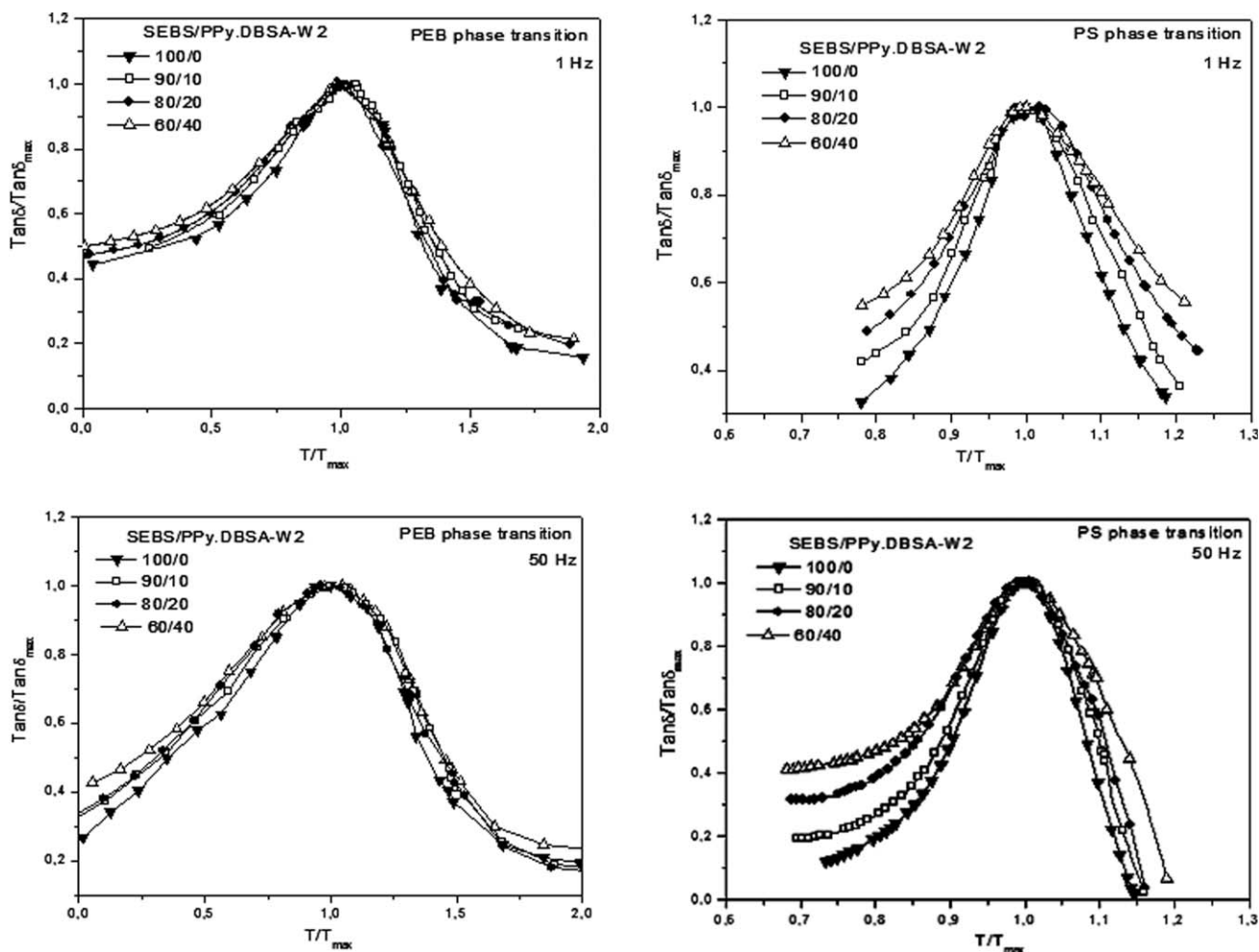


Figure 6 Normalized curves of $\tan \delta / \tan \delta_{\max}$ versus T/T_{\max} at 1 and 50 Hz for PEB and PS phase relaxations in undiluted SEBS and in SEBS/PPy.DBSA-W2.

no significant changes in the relative electrical conductivity were observed. For a filler content above 20 wt %, the conducting polymer particles are close, which contributes to an increase in the electrical conductivity of the blends. Under compressive stress, the contact between the conducting particles increases

TABLE II
Activation Energy of the Relaxation Process of PEB and PS Phases in the SEBS Matrix

Blend composition (wt %)	Activation energy (kcal mol ⁻¹)	
	PEB	PS
SEBS/PPy.DBSA-W1		
100/00	30	184
90/10	37	193
80/20	37	194
60/40	38	194
SEBS/PPy.DBSA-W2	(EB)	(S)
100/00	30	183
90/10	30	234
80/20	30	234
60/40	32	233

and, consequently, the relative electrical conductivity of the polymer blend increases significantly. For the blends with a conducting polymer content of 25 wt %, there was around a 36-fold increase in the relative conductivity with applied compressive stress of up to 6.0 MPa, reaching a constant value above this compressive stress [Fig. 8(a)]. Similar results were obtained for the blends with 30 wt % of conducting filler, although for these blends the compression sensitivity was around 2.1 MPa⁻¹, that is, there was around a 0.5-fold decrease compared with the blends with 25 wt % PPy.DBSA-W1 due to the greater number of conducting pathways in the latter. For a PPy.DBSA content of 40 wt %, there was only a 2.5-fold increase in the relative conductivity for the whole range of compressive stress. This behavior suggests that the PPy.DBSA particles are compact enough to allow the limit value of relative conductivity to be only slightly influenced by the compressive stress applied.

The SEBS/PPy.DBSA-W2 blends did not show a significant variation in the relative conductivity during the electromechanical assays, for the same

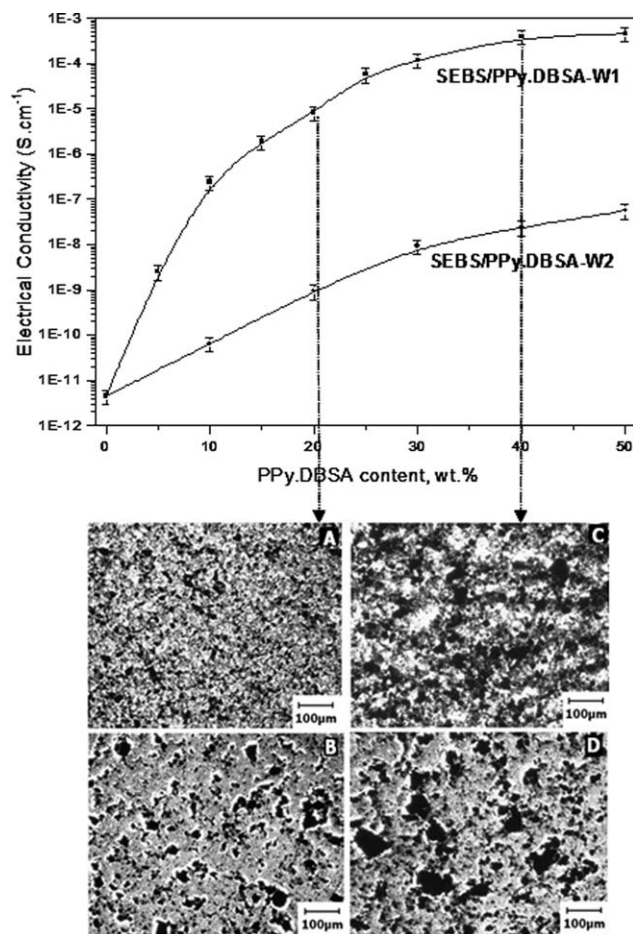


Figure 7 The effect of PPy.DBSA content on the electrical conductivity of SEBS/PPy.DBSA blends. Micrographs of (A, C) PPy.DBSA-W1 and (B, D) PPy.DBSA-W2 incorporated in SEBS matrix.

reason as that proposed for the SEBS/PPy.DBSA-W1 blends with a conducting polymer content below the percolation threshold (around 20 wt %). For these

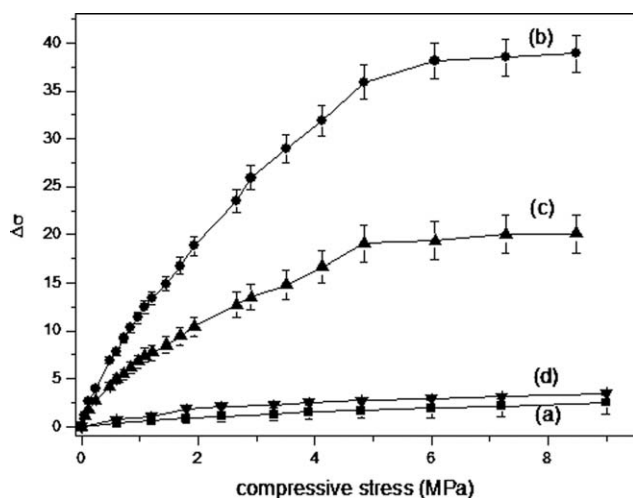


Figure 8 Relative conductivity ($\Delta\sigma$) as a function of applied pressure for SEBS/PPy.DBSA blends with (a) 20 wt %, (b) 25 wt %, (c) 30 wt %, and (d) 40 wt %.

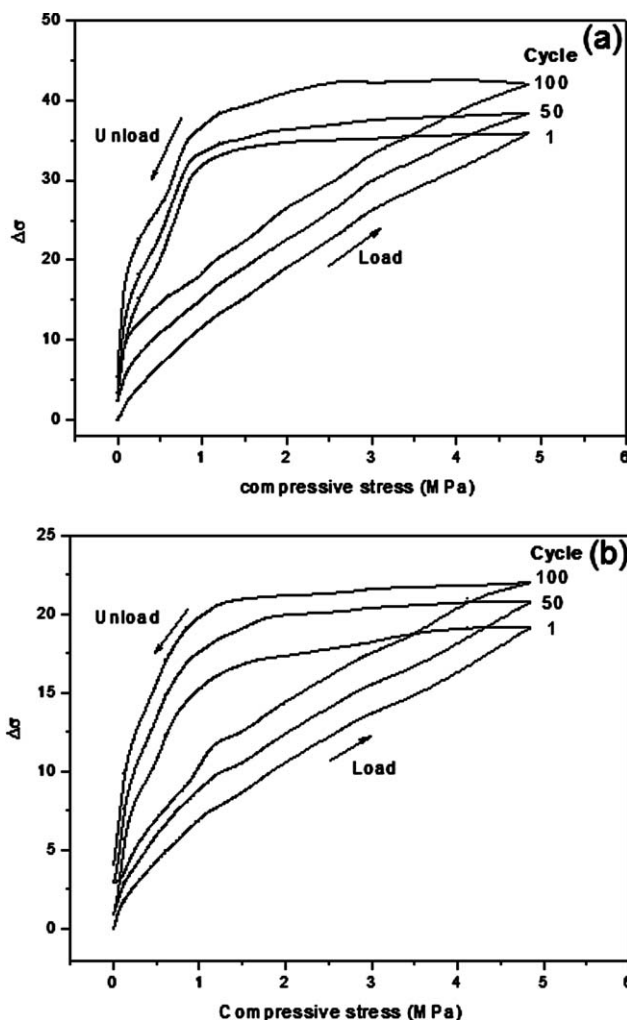


Figure 9 Relative conductivity ($\Delta\sigma$) as a function of load and unload cycle for SEBS/PPy.DBSA blends with (a) 25 wt % and (b) 30 wt %.

blends, a gross separated phase is observed and the conducting agglomerates are separated by a polymer matrix insulation layer and hence, the electrical conductivity is low in all compositions, even for 50 wt % of PPy.DBSA-W2 ($1.4 \times 10^{-8} \text{ S cm}^{-1}$). Similar behavior was observed by Hussain et al.⁹ for silicone/conductive carbon particle composites that show a conducting particle distribution and dispersion suitable for obtaining electrically conducting blends with high compression sensitivity.

The dependence of the relative conductivity on pressure during loading and unloading was measured for the blends, as can be seen in Figure 9. The irreversibility and hysteresis under mechanical stress are due to the breakdown of the conductive network or plastic deformation of the matrix. Thus, a slight difference between the final and initial relative conductivities, denominated the electrical set, in the cycles (1 to 100) can be observed for the blends with 25 and 30 wt % of PPy.DBSA-W1 content.

CONCLUSIONS

The characteristics of PPy.DBSA used to prepare conducting polymer blends with SEBS strongly affected the electrical conductivity, dynamic mechanical and electromechanical properties of the blends. The presence of free DBSA in the PPy.DBSA-W1 acts as a compatibilizing agent, inducing more dispersed conducting particles in the SEBS matrix. A heterogeneous microstructure was observed for SEBS/PPy.DBSA-W2 and lower electrical conductivity values were obtained compared with SEBS/PPy.DBSA-W1. The dynamic mechanical analysis showed that PPy.DBSA-W1 exhibits affinity for PEB and PS phases in the SEBS matrix, whereas PPy.DBSA-W2 presents more affinity with the PS phase. For the SEBS/PPy.DBSA-W1 blend specimens with 25 and 30% wt PPy.DBSA-W1 content, the compressive stress showed a considerable influence on the electrical conductivity and compressive sensitivity. The relative conductivity is almost the same as its previous value after the SEBS/PPy.DBSA-W1 sample loading is removed, which makes this material suitable for the development of pressure sensors.

References

1. Wang, Y.; Jing, X. *Polym Adv Technol* 2005, 16, 344.
2. Wang, H.-L.; Fu, C.-M.; Gopalan, A.; Wen, T.-C. *Thin Solid Film* 2004, 46, 6197.
3. Melo, C. P.; Neto, B. B.; Lima, E. G.; Lira, L. F. B.; Souza, J. E. G. *Sensor Actuator B* 2005, 109, 348.
4. Guimarda, N. K.; Gomez, N.; Schmidt C. E. *Prog Polym Sci* 2007, 32, 876.
5. Pyo, M.; Hwang, J.-H. *Synth Met* 2009, 159, 700.
6. Wu, Y.; Alici, G.; Madden, J. D. W.; Spinks, G. M.; Wallac, G. G. *Adv Funct Mater* 2007, 17, 3216.
7. Kalasad, M. N.; Gadyal, M. A.; Hiremath, R. K.; Ikram, I. M.; Mulimani, B. G.; Khazi, I. M.; Krishnan, S. K. A.; Rabinal, M. K. *Compos Sci Technol* 2008, 68, 1787.
8. Brady, S.; Diamond, D.; Lau, K.-T. *Sensor Actuator A* 2005, 119, 398.
9. Hussain, M.; Choa, Y.-H.; Niihara, K. *Compos Part A: Appl Sci Manufact* 2001, 32, 1689.
10. Sau, K. P.; Chaki, T. K.; Khastgir D. *Rubber Chem Technol* 2000, 73, 310.
11. Knite, M.; Teteris, V.; Kiploka, A.; Kaupuzs, J. *Sensor Actuator A: Phys* 2004, 110, 142.
12. Oliveira, F. A.; Alves, N.; Giacometti, J. A.; Constantino, C. J. L.; Mattoso, L. H. C.; Balan, A. M. O. A.; Job, A. E.; *J Appl Polym Sci* 2007, 106, 1001.
13. Soares, B. G.; Amorim, G. S.; Souza, F. G., Jr.; Oliveira, M.G.; Silva, J. E. P. *Synth Met* 2006, 156, 91.
14. Sau, K. P.; Chaki, T. K.; Khastgir, D. *J Appl Polym Sci* 1999, 71, 887.
15. Wang, P.; Ding T. *J Appl Polym Sci* 2010, 2035, 116.
16. Kost, J.; Foux, A. *Polym Eng Sci* 1983, 23, 567.
17. Vicentini, D. S.; Barra, G. M. O.; Bertolino, J. R.; Pires, A. T. N. *Eur Polym Mater* 2007, 43, 4565.
18. Barra, G. M. O.; Martins, R. R.; Kafer, K. A.; Paniago, R.; Vasques, C. T.; Pires, A. T. N. *Polymer Testing* 2008, 27, 886.
19. Souza, F. G., Jr.; Soares, B. G.; Siddaramaiah; Barra, G. M. O.; Herbst, M. H. *Polymer* 2006, 47, 7548.
20. Wang, J.; Yang, W.; Tong, P.; Lei, J. *J Appl Polym Sci* 2009, 115, 1886.
21. Ruangchuay, L.; Sirivat, A.; Schwank, J. *Talanta* 2003, 60, 25.
22. Lee, J. Y.; Kim, D. Y.; Kim, C. Y. *Synth Met* 1995, 74, 103.
23. Joo, J.; Lee, J. K.; Lee, S. Y.; Jang, K. S.; Oh, E. J.; Epstein, A. J. *Macromolecules* 2000, 33, 5131.
24. Ge, H.; Qi, G.; Kang, En-T.; Neoh, K. G. *Polymer* 1994, 35, 504.
25. Leyva, M. E.; Soares, B. G.; Khastgir, D. *Polymer* 2002, 43, 7505.
26. Leyva, M. E.; Barra, G. M. O.; Moreira, A. C. F.; Soares, B. G.; Khastgir, D. *J Polym Sci Part B: Polym Phys* 2002, 41, 2983.
27. Olabisi, O.; Robeson, L. M.; Shaw, M. T. *Polymer-Polymer Miscibility*. Academic Press: New York, 1979; Chapter 5, p 219.
28. Levon, K.; Margolina, A. *Macromolecules* 1993, 26, 4061.